EQPH-2021
V. International Symposium
Proceedings Book of the Vth International Symposium–2021
"Environmental Quality and Public Health"
May 20, 2021 Óbuda University, Budapest, Hungary
ISBN: 978-963-449-238-2. **www.iceee.hu**
KL2.

CHARACTERIZATION OF GEOSYNTHETICS AT VARIOUS ENVIRONMENTAL CONDITIONS

Abdelwahab Tahsin*[1], Rami El-Sherbiny[2]

*[1]*Civil Engineering Department/ Cairo University, Cairo, Egypt, e-mail: abdelwahab.tahsin@gmail.com, mobile: +201001729119*

Abstract: *In the last two decades, geosynthetics became a common application in Geoenvironmental engineering. Use of geosynthetics as a sustainable construction solution in civil engineering was reported by the Waste and Resources Action Program (WRAP, 2010), presenting case studies of sludge lagoon, tailing ponds and soil waste systems, wherein geosynthetic introduced reduction in cost and CO_2 emission. Geosynthetics enhance the soil quality, performance, strength parameters, and regularly pragmatic as a soil reinforcement in the exhibition of high loads while strengthening of tailing impoundments and landfills. It is an appropriate soil improvement system with unique advantages compared to other conventional ones. This manuscript introduces analyses and results of laboratory constant strain rate (CSR) test of 20%, 10%, 6%, 3%, 1% and 0.05% strain/min conducted on five specimens of geosynthetics polyester (PET) geogrids. Tests were performed according to the Multi-Rib tensile method of ASTM D6637. Main output acceptance features of tensile ultimate strength and the strain at break were justified. Stiffnesses at strain of 1% and 2% were derived. Sensitivity of strain rate of loading on strength, stiffness and non-linear properties of geogrid was inspected. Results of the measured tensile load-strain relationship for working are loads (strain ≤ 2%) and considerably acknowledged of linear simulation. The larger ultimate strength, the higher anticipated stiffness irrespective to loading strain rate. The derived stiffness at 1% is larger than corresponding for 2% strain, which reflects phenomenon of non-linearity and stiffness relaxation with progressive elongation. Behavior of reinforced soil is sensitive to stiffness rather than strength of geogrid.*

Keywords: *constant strain rate test, geosynthetics, non-linear, soil improvement, stiffness, strength*

INTRODUCTION

In the last two decades, geosynthetics became a common application in Geoenvironmental engineering. Use of geosynthetics as a sustainable construction solution in civil engineering was reported by the Waste and Resources Action Program (WRAP, 2010), presenting case studies of sludge lagoon, tailing ponds and soil waste systems, wherein geosynthetic introduced reduction in cost and CO_2 emission. Geosynthetics enhance the soil quality, performance, strength parameters, and regularly pragmatic as a soil reinforcement in the exhibition of high loads while strengthening of tailing impoundments and landfills. It is an appropriate soil improvement system with unique advantages compared to other conventional ones.

Hypostatically, the behavior of geosynthetic reinforced soil is complicated due to the mechanical complexity of component materials, their interactions, geosynthetic properties, and soil characteristics as well. Numerical modelling of geosynthetic reinforced soil systems is now extensively utilized for

the design, prediction of measured responses, and in research to generate synthetic data for the purpose of filling-in knowledge gaps on the behavior of these systems. (Yu and Bathurst, 2016).
In the engineering community, the available technical data sheets promoted by the geosynthetics manufacturers include only key design features of the ultimate strength and strain at break. On the contrary, the information about stiffness and secant modulus are not disclosed. These stiffness data are essential key input parameters for numerical modelling (Finite Element Method). Also, the non-linear stress-strain relationship of the geosynthetics is necessary to be investigated by conducting series of laboratory tensile test, perform date interpretation of the measured test results and identify the secant modulus at various strain domains.
In this research paper work, we are focused on conducting proper geosynthetics characterization necessary for numerical simulations that can be used to predict operational (working stress) conditions rather than incipient wall collapse. A contribution of such undertaken proper material characterization of geosynthetics is essential for numerical finite element modelling for multi- asset application of geosynthetics reinforced soils such as: (a) soil reinforcement in the exhibition of high loads while strengthening of tailing impoundments and landfills, (a) soil improvement in general applications, (c) slope stability deemed to achieve the stability of sharp slopes in the presence of low shear strength deposits, and (d) mechanically stabilized earth wall to act as an efficient retaining system in an economical design basis.

MATERIALS AND METHODS

a. OVERVIEW

The current study comprises 5 sets of nominated specimens Fortrac 35T, 55T, 80T, 110T, and 150T with varying strength and stiffness. Table 1 listed the physical properties of geogrid types as per the technical data sheet introduced by the manufacturer HUSKER. The standard raw material of these geogrids is the high-modulus polyester (PET), which of high stiffness, low creep and uniform product strength.
The geogrid specimens were tested on a tensile test machine under Constant Strain Rate (CSR) test in accordance with ASTM D6637, to investigate: (a) Tensile ultimate strength KN/m, and (b) strain at break. The secant modulus (J) KN/m at strain of 1% and 2% were derived based on the tensile force-strain relationship which is necessary for numerical modelling simulation. The CSR was varied to study the effect of strain rate of loading on the tensile strength and stiffness of the examined specimens of the PET geogrid.

Table 1: Physical properties for the tested geogrid types as per HUSKER data sheets

PROPERTY	TEST	**35T**	**55T**	**80T**	**110T**	**150T**
Mass/Unit Area (g/m^2)	ASTM D-5261	185	240	320	350	440
Aperture Size (mm)	measured	25 x 25	25 x 25	25 x 25	25 x 25	25 x 25
Percent open area	CWO 22125	70%	70%	65%	65%	62%
Ultimate wide width (MD) Tensile Strength (kN/m)	ASTM D-6637	**35**	**55**	**80**	**110**	**150**
Elongation at ultimate tensile strength –MD	ASTM D-6637	≤10%	≤10%	≤10%	≤10%	≤10%
Long term design strength- MD (kN/m)*	GRI GG4	18.8	29.5	42.9	59	81
Standard Roll Size (m)		5x100	5x100	5x100	5x100	5x100
Weight (kg)		114	141	182	192	205

* To be reduced by factors: Durability = 1.2 and Installation= 1.2.

b. TEST APPARATUS AND SPECIMEN PREPARATION

TESTOMETRIC M500- 50CT Universal Testing machine was used to perform the geogrid load-extension under Constant Strain Rate CSR. The apparatus comprises main tensile machine, pressure jack and computer control unit. The tensile machine consists mainly of clamps, sensors for recording the tensile force, and other sensors to monitor the extent of grips separation. The clamps must be attached with suitable pressure to avoid slippage. Clamping pressure must be equal for all specimens under the same test to manage consistent judgment between the anticipated results. Figure (1) presents photo of the tensile test apparatus and specimen installation prior to start of strain loadings. According to the Multi-Rib tensile method of ASTM D6637 "Standard Test Method for Determining Tensile Properties of Geogrids by the Single or Multi-Rib Tensile Method"; the specimen is schematically illustrated at Figure (2) should be a minimum of 200 mm wide and contains five ribs in the cross-test direction by at least three junctions or 300 mm long in the direction of the testing. The outermost ribs are cut prior to testing to prevent slippage from occurring within the clamps as instructed by ASTM D6637, clause 8.2.4. Thus, the width of intact ribs is 120 mm. The room ambient temperature was 20°c during test procedures to avoid adverse impact of the temperature in the test results.

Figure (1): Constant Strain Rate CSR tensile test apparatus

Figure (2): Specimen configuration; Multi-Rib tensile method -ASTM D6637

STATISTICAL ANALYSIS AND GRAPHICAL PRESENTATION

Minimum of three to five single tests were performed on the Machine Direction (MD) for each specimen of Fortrac 35T, 55T, 80T, 110T, and 150T, in accordance with ASTM D6637 using the multi- rib tensile method. Wide scatter of Constant Strain Rate CSR of 20%, 10%, 6%, 3%, 1% to slow rate loading 0.05% strain/min. were performed. The CSR was varied to study the effect of strain rate of loading on the tensile strength and stiffness of the PET geogrid.

The tensile test results are necessary to address the main output acceptance features: (a) tensile ultimate strength kN/m, and (b) strain at break. The secant modulus (J) kN/m at strain of 1% and 2% were derived based on the tensile force- strain relationship which is necessary for numerical modelling simulation. Since the geogrid CSR tests were carried out at the same in-door ambient temperature of 20°C, temperature effect was not a factor in the test results accuracy.

RESULTS AND DISCUSSION

a. Tensile load versus strain test results

In accordance with ASTM D 4595 and after Hatami and Bathurst 2005; the determination of the ultimate strength is established on the peak strength measured during CSR of 10% strain/min. Based on the test measurement results, the Tensile Strength (kN) was derived by dividing the measured Peak Force by the width of intact ribs (120 mm). The Secant modulus kN/m at strain 2% was calculated by dividing the measured tensile force (at strain 2%) by 120 mm to get the tensile stresses then divided by 0.02 strain to result in the stiffness (secant modulus $J_{2\%}$).
A range of 1.92-1.75 was derived for Factor of Safety FOS which is safely covered the deemed long term strength as well as durability and installation factors (reductions) with wide acceptable margin as shown at Table 2. This FOS is calculated by dividing the mean measured tensile strength of the CSR tests listed in Table 2 by the long term design strength listed in Table 1 "physical properties of the examined geogrid as per the technical data sheet". For example for 110T; FOS= 112.73/59.0= 1.92. Hence, results are in good agreement with manufactures technical data sheet.
The linear approximation of tensile load- strain response is considerable accepted in the strain domain up to 2% which covers a wide scatter of geosynthetics reinforced structures conditions under service (working) loadings. Sample of the test results for five single specimens at 20% /min of 35T, 55T, 80T, and 110T are presented at Figure (3).

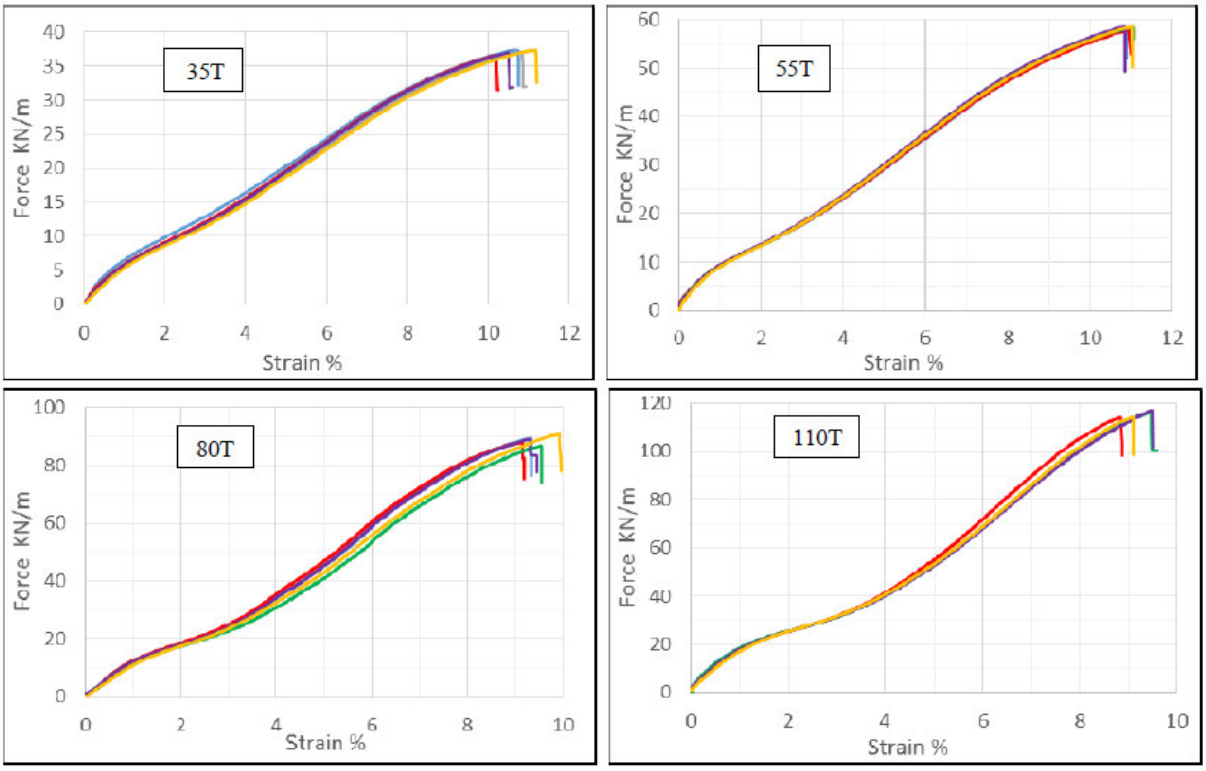

Figure (3): Force- strain response at CSR 20 %/min for the tested specimens of Fortrac 35T, 55T, 80T, and 110T

Table 2: CSR test results for 10% strain/min- ASTM D 4595

Type	Test	Peak Force (kN)	Tensile strength (kN/m)	Secant modulus kN/m (strain 2%)	Strain at peak %
35T	1	4.30	35.85	384	10.3
	2	4.41	36.74	377	10.6
	3	3.87	32.27	395	9.5
	4	4.21	35.07	389	10.3
	5	3.77	31.44	403	9.0
	mean	4.11	34.27	390	9.9
55T	1	7.23	60.28	546	11.5
	2	7.08	58.98	528	11.4
	3	6.12	51.03	512	10.7
	4	6.05	50.43	537	9.6
	5	6.10	50.83	558	10.8
	mean	6.52	54.31	536	10.8
80T	1	11.06	92.19	859	11.1
	2	9.69	80.75	822	10.0
	3	10.95	91.24	854	11.0
	4	8.81	73.42	923	9.9
	5	8.09	67.42	883	8.3
	mean	9.72	81.00	868	10.1
110T	1	15.7	130.83	1099	11.9
	2	15.08	125.67	1126	11.2
	3	14.06	117.13	1095	10.8
	4	11.48	95.67	1165	9.1
	5	11.32	94.33	1153	8.9
	mean	13.53	112.73	1128	10.4

b. Influence of strain loading rate on strength

The CSR was varied at rates 20%/min, 10%/min, 6%/min, 3%/min, 1%/min, and 0.05%/min to study the effect of strain rate of loading on the tensile strength and stiffness of the examined PET geogrid specimens. The influence of CSR on the tensile force- strain relationship and ultimate strength is illustrated in Figure 4 for the different geogrid examined specimens at rates 10%/min, 6%/min, 3%/min, and 1%/min where, the recorded tensile load increased as the CSR increased. The slow-rate rate 0.05%/min. was not conducted to the failure, as it consumed long time to reach the peak strain associated with failure. Testing was completed to approximate of 3% strain which cover wide range of the anticipated strain for service loading for various types of geosynthetic reinforced soil applications. Hence, the secant modulus at strain 2% was calculated accordingly.

Results show that, the higher CSR reveals increase of the measured secant modulus. The larger ultimate strength, the higher anticipated stiffness irrespective to loading strain rate. Based on the measured tensile load- strain relationship, the linear approximation of secant modulus is considerably acknowledged in the strain domain $\leq$ 2% which covers a wide scatter of geosynthetics reinforced structures conditions under service (working) loadings. Behavior of geosynthetics reinforced soil is sensitive to stiffness rather than strength of the geogrid.

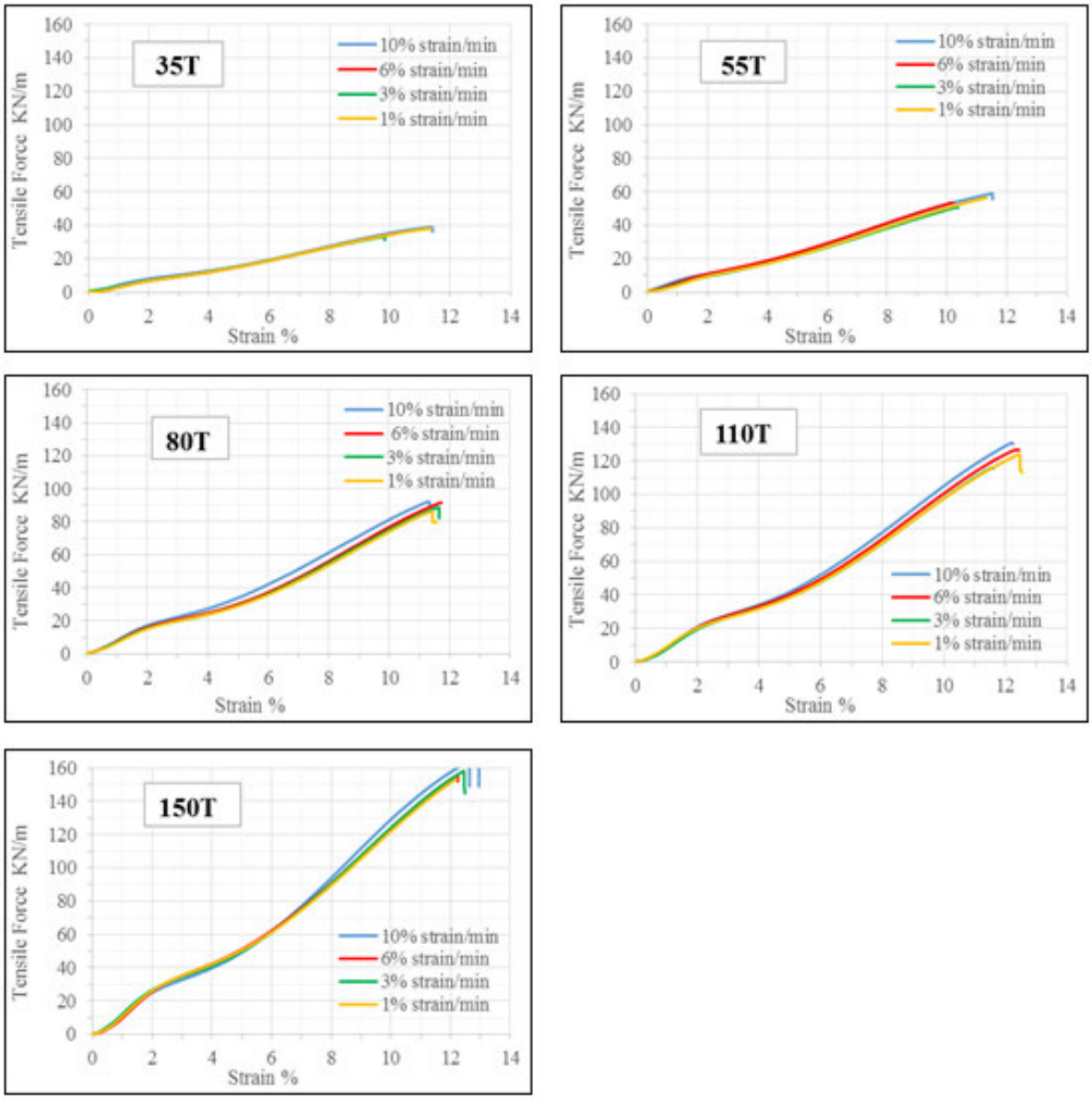

Figure (4): Influence of strain rate of 10, 6, 3 and 1%/min. on tensile force-strain relationship for Fortrac 35T, 55T, 80T, 110T, and 150T

c. Secant modulus (stiffness)

The sample total width is 200 mm, while the intact width is limited to 120 mm. According to ASTM D6637, clause 8.2.4 which stated that "within test methods A, B and C the outermost ribs are cut prior to testing to prevent slippage from occurring within the clamps. For those cases where the outermost ribs are severed, the test results shall be based on the unit of width associated with the number of intact ribs". Hence, calculation of the secant modulus ($J = EA_1$) at certain strain domain shall be the maximum tensile force divided by the total intact width per meter. The strength and stiffness of the geogrid is load, time, and temperature dependent. The room temperature is to be 20°c during testing procedure to avoid adverse influence of temperature on the test results. The literature (Boyle et al., 1996; Sawicki et al., 2002; Walters et al., 2002), stated that the geogrid is affected by strain rate of loading. After Hatami and Bathurst (2005), the determination of the ultimate strength, characteristics, and secant modulus are based on the results of CSR for 10% strain/min- ASTM D4595.
Accordingly, at CSR 10%/min., the derived secant moduli for stain domain of 2% are 390, 536, 868, 1128 and 1396 kN/m for types 35T, 55T, 80T, 110T and 150T, respectively. The resulting secant moduli for strain domain up to 1% are 521, 729, 1104, 1583, and 1583 kN/m for specimens 35T, 55T,

80T, 110T and 150T, respectively. Figure (5) demonstrates the trend between ultimate tensile strength for the examined specimens of Fortrac 35T, 55T, 80T, 110T, and 150T under CSR 10%/min. and the resultant secant modulus $J_{2\%}$ for strain domain 2% as well as secant modulus $J_{1\%}$ for strain domain 1%. For all examined geogrid specimens, the revealed modulus at domain 1% is relatively larger than corresponding for strain domain 2%, which reflects the phenomenon of the non-linearity and relaxation of geogrid stiffness with progressive elongation (strains). The higher induced strain, the relatively lower anticipated stiffness is. As reported by Hatami and Bathurst 2005, the linear approximation of tensile load- strain response is considerable accepted in the strain domain up to 2% which covers a wide scatter of geosynthetics reinforced soil/ structures conditions under service loadings rather than the incipient collapse.

It should be pointed that, the performance of geosynthetic reinforced structure is sensitive to the geogrid stiffness rather than the geogrid strength. Values for secant modulus J at strain level 1% and 2% which were derived from the CSR tensile force- strain relationship results are utilized for derivation of the brought geogrid tensile forces based on the measured strains of the instrumented geogrid layers. Secant modulus of strain 2% is a necessary key input parameter for numerical finite element modelling of geogrid properties.

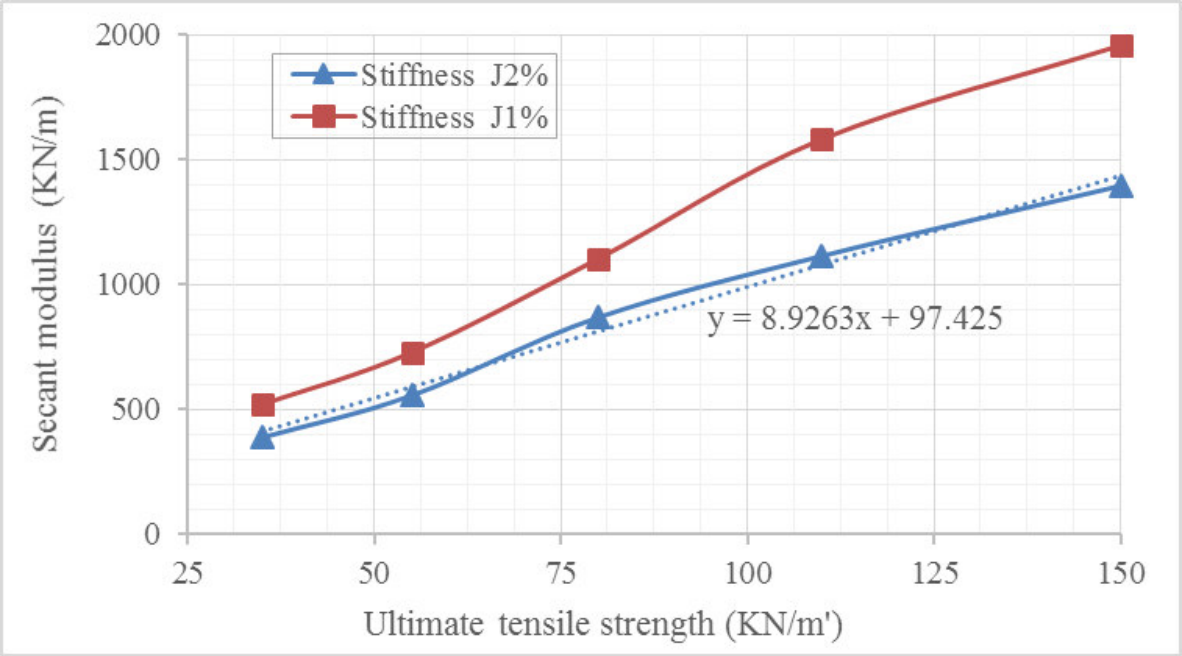

Figure (5): Trend of ultimate tensile strength versus secant modulus $J_{2\%}$ and $J_{1\%}$ for CSR 10%/min.

The performed CRS tests program did not involve testing of specimen 200T. Thus, correlated to the examined specimens CSR test results of 35T, 55T, 80T, 110T and 150T, a statistical prediction for the trend among strength, secant modulus $J_{2\%}$ at 2% strain and $J_{1\%}$ at 1% strain was used to estimate the secant modulus $J_{1\%}$ and $J_{2\%}$ of Fortrac 200 of value 2538 kN/m and 1893 kN/m, respectively. Ratios between stiffness ($J_{2\%}$) to stiffness ($J_{1\%}$) for various examined specimens and predicted stiffness values of Fortrac 200T were evaluated as presented in Table 3, where the predicted (fitted) secant modulus $J_{2\%}$ = 8.9263 x Ultimate Tensile Strength + 97.425.

From a practical stand point, such expression and chart (correlation) are simple and helpful to predict secant modulus (not published by manufactures to public engineering community) of geosynthetic PET geogrid based on nominal ultimate strength, which is essential key input parameter for numerical FE modelling purposes.

Table 3: CSR test for 10% strain/min. – secant modulus $J_{2\%}$ and $J_{1\%}$

	Tested specimens					Predicted
	35T	55T	80T	110T	150T	200T
Measured $J_{2\%}$ (kN/m)	390	536	868	1128	1396	
Fitted $J_{2\%}$ (kN/m)	410	588	812	1079	1436	1893
diff. (kN/m)	5.09	9.77	-6.51	-4.32	2.89	
Measured $J_{1\%}$ (kN/m)	521	729	1104	1583	1958	2538.9 (fitted)
$J_{1\%}$/ $J_{2\%}$ ratio	1.336	1.360	1.272	1.403	1.403	average = 1.355

The CSR was varied to assess the effect of strain rate of loading of 20%/min, 10%/min, 6%/min, 3%/min, %/min and 0.05%/min. on the secant modulus at strain 2% ($J_{2\%}$) and at strain 1% ($J_{1\%}$) as illustrated in Figures. 6 and 7, respectively.

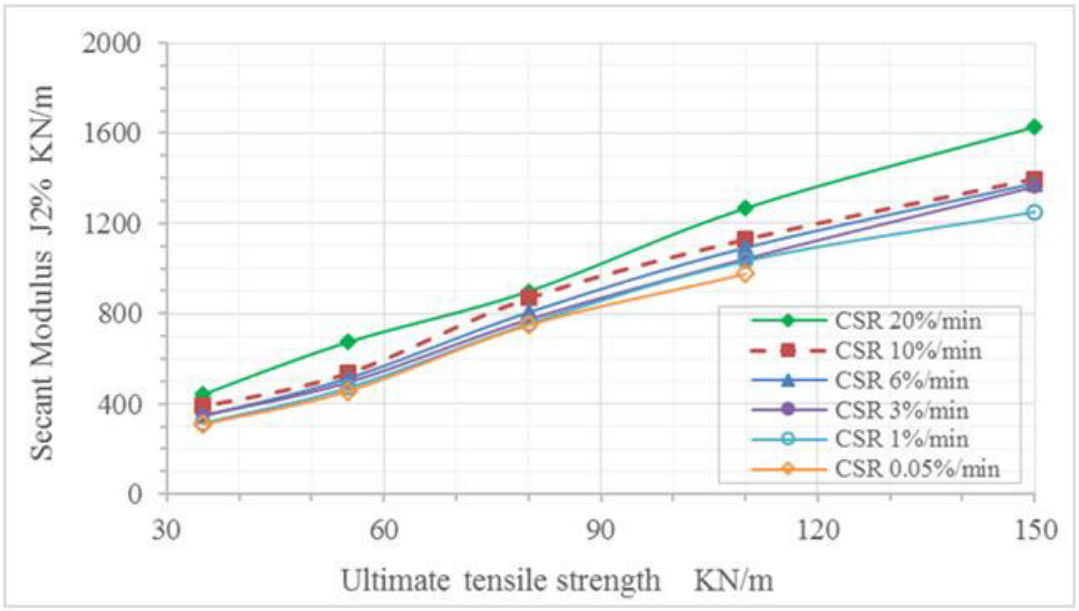

Figure (6): Influence of strain rate of 20, 10, 6, 3, 1 and 0.05 %/min. on geogrid secant modulus J2%

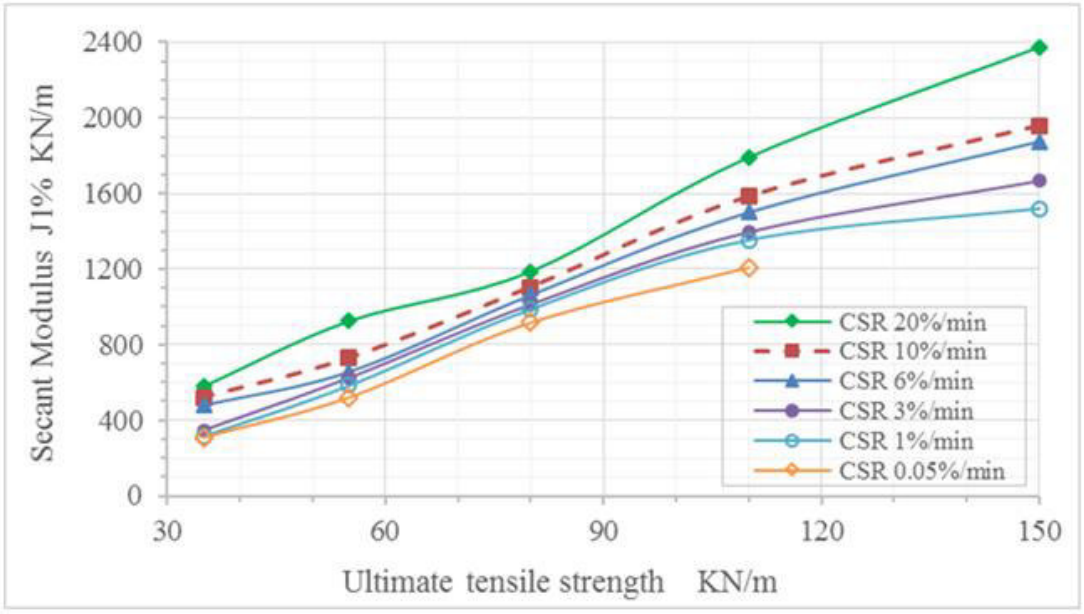

Figure (7): Influence of strain rate of 20, 10, 6, 3, 1 and 0.05 %/min. on geogrid secant modulus J1%

General trend of the test results shows that, the larger ultimate strength, the higher anticipated secant moduli, regardless of the strain rate of loading. For the different examined geogrid specimens, the higher CSR reveals an increase of the induced secant modulus J2% and J1% for the same examined specimen with variable ratios.
For practical assessment of the influence for strain rate of loading, the anticipated secant modulus for the examined specimens shall be normalized to the corresponding of the nominal representative test of rate 10%/min. of ASTM D4595 (after Hatami and Bathurst 2005).
Table 4 listed the normalized ratios of the variable strain loading rates to rate 10%/min. of $J_{2\%}$. For example; increasing rate to the upper bound (fast loading rate) 20 %/min provided an increased ratio of $J_{2\%}$ from 1.03 to 1.26. On the contrary, reducing rate to the lower bound (slow loading rate) 0.05 %/min. exposed a decreased ratio of $J_{2\%}$ from 0.80 to 0.87.

Table 4: Influence of CSR at modulus $J_{2\%}$ -normalized to 10% strain/min.

	CSR 20%/min.	CSR 6%/min	CSR 3%/min	CSR 1%/min	CSR 0.05%/min
150T	1.17	0.99	0.98	0.90	
110T	1.12	0.97	0.92	0.92	0.87
80T	1.03	0.93	0.89	0.87	0.86
55T	1.26	0.96	0.92	0.88	0.85
35T	1.13	0.89	0.89	0.81	0.80

Table 5 shows the normalized ratios of the variable strain loading rates to rate 10%/min. of secant modules $J_{1\%}$. For example; increasing rate to the upper bound (fast loading rate) 20 %/min provided an increased ratio of $J_{1\%}$ from 1.08 to 1.27. In contrast, decreasing rate to the lower bound (slow loading rate) 0.05 %/min. exposed a reduced ratio of $J_{1\%}$ ranged from 0.71 to 0.83.

Table 5: Influence of CSR at modulus J1%- normalized to 10% strain/min.

	CSR 20%/min.	CSR 6%/min	CSR 3%/min	CSR 1%/min	CSR 0.05%/min
150T	1.21	0.96	0.85	0.78	
110T	1.13	0.95	0.88	0.86	0.76
80T	1.08	0.96	0.92	0.89	0.83
55T	1.27	0.90	0.86	0.80	0.71
35T	1.11	0.92	0.88	0.76	0.76

CONCLUSIONS AND RECOMMENDATIONS

This manuscript introduces analyses, interpretation and results for series of laboratory constant strain rate (CSR) tests of 20%, 10%, 6%, 3%, 1% and 0.05% strain/ min. conducted on five sets of geosynthetics polyester (PET) geogrid specimens. Tests were performed according to the Multi-Rib tensile method of ASTM D6637. Main output acceptance features of tensile ultimate strength and strain at break was justified. Results are in good agreement with manufactures technical data sheet. Values for Secant modulus J at strain level 1% and 2% were derived from the tensile force- strain relationship results, which are necessary for numerical Finite Element modelling. Sensitivity for the influence of strain rate of loading on strength, stiffness and non-linear properties of geogrid was inspected for the different examined specimens. We are focused on simulations that can be used to predict operational (working stress) under static conditions rather than incipient collapse.
The main findings might be summarized as follows:

- The measured tensile force –strain relationship showed a non-linear behavior of the examined geosynthetics PET geogrid.

- The higher CSR reveals increase of the measured secant modulus. The larger ultimate strength, the higher anticipated stiffness irrespective to loading strain rate.
- Based on the measured tensile load- strain relationship, the linear approximation of secant modulus is considerably acknowledged in the strain domain ≤ 2% which covers a wide scatter of geosynthetics reinforced structures conditions under service (working) loadings.
- The derived stiffness at 1% is larger than corresponding for 2% strain, which reflects phenomenon of non-linearity and stiffness relaxation with progressive elongation.
- Behavior of reinforced soil is sensitive to stiffness rather than strength of geogrid.
- For numerical modelling purposes, a simple correlation chart was developed to predict secant modulus (not published to public) of geosynthetic PET geogrid based on the ultimate strength.
- For practical assessment of the influence for strain rate of loading on stiffness; tables were developed for the normalized ratios to rate of 10% strain/min. (ASTM D4595) for $J_{2\%}$ and $J_{1\%}$.

ACKNOWLEDGEMENT

The authors would like to express their gratitude to the technical support of Dr. Mohy El-Mashad, and members of Geotechnical Institute Laboratory, National Irrigation Research Center in Qanater, Egypt.

REFERENCES

1. AASHTO (2002). Standard Specifications for Highway Bridges. American Association of State Highway and Transportation Officials, 17th Ed., Washington, DC, USA.
2. Allen, T. M., and Bathurst, R. J. (2002a). “Observed long-term performance of geosynthetic walls, and implications for design.” Geosynthetic Int., 9(5–6), 567–606.
3. ASTM D 6637. "Standard test method for determining tensile properties of geogrids by the single or multi-rib tensile method." American Society for Testing and Materials, Pennsylvania, USA.
4. ASTM D4595 "Standard test method for tensile properties of geotextiles by the wide-width strip method." American Society for Testing and Materials, West Conshohocken, Pennsylvania, USA
5. Bathurst, R.J., Allen, T.M., and Walters, D.L., (2002), “Short-term strain and deformation behaviour of geosynthetic walls at working stress conditions”, geosynthetics international, vol. 9, nos. 5-6, pp. 451-482.
6. Boyle, S.R, Gallagherand, M. Holtz, R.D. (1996). “Influence of strain rate, specimen length and confinement on measured geotextile properties.” Geosynthetics International Journal, 3 (2), pp. 205-225.
7. Hatami, K. and Bathurst, R. J. (2005). “Development and verification of a numerical model for the analysis of geosynthetic-reinforced soil segmental walls under working stress conditions.” Journal of Geotechnical and Geoenvironmental Engineering, ASCE, 132(6), 673 684.
8. Niall C., Patrick C., Sophie N., and Andrew T., Waste and Resources Action Program WRAP (2010). “Sustainable geosystems in civil engineering applications”. http://www.wrap.org.uk
9. Yan Yu, Bathurst, R. J., and Allen, T. M. (2016). “Numerical modelling of the SR-18 geogrid reinforced modular block retaining walls.” Journal of Geotechnical and Geoenvironmental Engineering, ASCE, 142 (5): 04016003.
10. Sawicki, A., and Kazimierowicz-Frankowska, K. (2002). “Influence of strain rate on the load-strain characteristics of geosynthetics.” Journal of Geosynthetics International, 9 (1), pp. 1-19
11. Walters, D. L., Allen, T. M., & Bathurst, R. J. (2002). “Conversion of geosynthetic strain to load using reinforcement stiffness.” Geosynthetics International, 9 (5-6), pp. 483-523.